Epitaxial Ferroelectric Thin Films on Silicon Substrates for Future Electronic Devices

●Masao Kondo ●Kenji Maruyama ●Kazuaki Kurihara

(Manuscript received January 25, 2002)

A lead lanthanum zirconate titanate ($(Pb_{1-2/3y}La_y)(Zr_{1-x}Ti_x)O_3$, PLZT) thin film with a thin-film bottom electrode of strontium ruthenium oxide ($SrRuO_3$, SRO) can be grown epitaxially on a (001) silicon substrate. Ceria (CeO_2) and yttria-stabilized zirconia (YSZ) were used as a buffer layer. This paper discusses the orientation and domain structure of PLZT thin films on an SRO/CeO_2/YSZ buffer layer. All oxide thin films of the PLZT/SRO/CeO_2/YSZ heteroepitaxial structure were oriented toward (001). The CeO_2 and YSZ grew epitaxially with a cube-on-cube alignment with the diamond structure of the silicon. The PLZT and SRO thin film rotates 45° in-plane with respect to the fluorite structure of CeO_2. The remanent polarization of a $PbLa_{0.03}Zr_{0.45}Ti_{0.55}O_3$ epitaxial thin film is 10 μC/cm² and is smaller than that of a (001)-oriented epitaxial PLZT thin film with a platinum bottom electrode on a magnesia (MgO) substrate. The profiles of the reciprocal space mapping reveal that the PLZT epitaxial thin films were distorted into a pseudocubic structure by the tensile stress from the silicon substrate.

1. Introduction

Ferroelectric thin films have attracted much interest, both from the fundamental and applied aspects. These films are used in, for example, ferroelectric random access memories (FeRAMs), piezoelectric actuators, micro-electro-mechanical systems (MEMS), and pyroelectric detectors. $Pb(Zr_xT_{i-x})O_3$ (PZT) and $(Pb_{1-2/3y},La_y)(Zr_{1-x},Ti_x)O_3$ (PLZT) are promising materials for use as ferroelectric thin films. PZT thin films have already been prepared by several methods, for example, sputtering, metal organic chemical vapor deposition, chemical solution deposition, and pulsed laser deposition (PLD). PLD is a suitable method for preparing highly oriented multicomponent thin films. Using PLD, it is easy to transfer the stoichiometric composition of components, including volatile elements such as lead and bismuth, from the target to the thin film. Furthermore, it is also easy to realize multilayer structures if the targets are changed during the deposition process.

Epitaxial growth of thin films on a silicon substrate is considered to be a key technology for fabricating even thinner and smaller electronic devices in the future, because their leakage current and optical scattering are expected to be lower than those of polycrystalline films.[1] These features are important for applications in devices such as metal-ferroelectric-semiconductor-field effect transistors (MFS-FETs),[2] optical devices, and so on.[1]

However, the epitaxial growth of oxide thin films on a silicon substrate has some basic problems.[3),4] First, the surface of the silicon is easily oxidized into amorphous silicon oxide by the oxygen in oxide films or the ambient atmosphere. No epitaxial oxide thin film can be prepared on the amorphous silicon oxide, because it cannot continue the crystallinity of the silicon. Secondly, most of the cations in the oxide film easily diffuse

into the silicon substrate or react with the silicon. The secondary phase formed by diffusions or reactions disturbs the crystallinity of the silicon. Thus, an essential characteristic for epitaxial growth of an oxide thin film on a silicon substrate is low reactivity with silicon. Some typical oxides are alumina (Al_2O_3),[5] magnesia (MgO),[6),7] and yittria-stabilized zirconia (YSZ).[8]

YSZ thin film grows epitaxially on a silicon substrate. The epitaxial relationship between YSZ and silicon is (001) of YSZ ∥ (001) of silicon and (100) of YSZ ∥ (100) of silicon (cube-on-cube alignment).[3] Perovskite compounds such as barium strontium titanate ((Ba,Sr)TiO_3) and strontium ruthenium oxide ($SrRuO_3$, SRO) are also grown epitaxially on YSZ thin film. However, the epitaxial relationships between YSZ and these perovskite compounds are (011) of perovskite ∥ (001) of YSZ.[9] The polarization direction of a ferroelectric perovskite compound with a tetragonal phase is (001). This indicates that the polarization of ferroelectric perovskite is rotated 45° with respect to the substrate surface. The polarization of a (011)-oriented perovskite thin film is smaller than that of a (001)-oriented one.

Ceria (CeO_2) also grows epitaxially with the cube-on-cube alignment on a YSZ thin film.[10),11] Recently, the CeO_2/YSZ double buffer layer has attracted much interest, because perovskite thin films orient toward the (001) direction on a CeO_2 thin film. Electrode materials with a perovskite structure, such as ($La_{0.5}$,$Sr_{0.5}$)CoO_3 (LSCO) and $YBa_2Cu_3O_{7-\delta}$ (YBCO) have been prepared on a CeO_2/YSZ double buffer layer on a silicon substrate.[10),12)-15]

Strontium ruthenium oxide ($SrRuO_3$, SRO) is promising as an electrode material because it has a simple perovskite structure. Another advantage for YBCO and LSCO is the controllability of the composition during the deposition process, because SRO consists of three elements. The epitaxial growth of SRO on a CeO_2/YSZ buffer layer has not been investigated fully. Furthermore, the domain structure, orientation, and polarization of an epitaxial PLZT thin film on SRO/CeO_2/YSZ heteroepitaxial structures on a silicon substrate are unclear.

In this paper, we describe how we formed a PLZT/SRO/CeO_2/YSZ/Si heteroepitaxial structure by the PLD method. We also discuss the relationship between the domain structure and the polarization property of the PLZT thin film.

2. Experimental procedure

First, we cleaned 2-inch (001) silicon wafers with dilute HF acid to remove the amorphous SiO_2 layers on the surface. The YSZ, CeO_2, and SRO buffer layers were deposited by pulsed laser deposition. The wavelength of the KrF excimer laser was 248 nm. Ceramics of 8 mol% Y_2O_3-doped ZrO_2, CeO_2, and SRO with a 99.9% purity were used as targets. The depositions were carried out in 7.3×10^{-2} Pa under an oxygen flow at 740°C. The final thicknesses of the YSZ, CeO_2, and SRO were around 30, 30, and 100 nm, respectively.

The PLZT thin films were prepared on the SRO/CeO_2/YSZ thin films on a silicon substrate by a chemical solution method. The solution compositions were $Pb_{1.13}La_{0.03}Zr_{0.45}Ti_{0.55}O_3$ and $Pb_{1.13}La_{0.03}Zr_{0.2}Ti_{0.8}O_3$ (hereafter PLZT3/45/55 and PLZT3/20/80, respectively). The coated SRO/CeO_2/YSZ silicon wafers were heated by a hot plate at 350°C after spin coating. This process was repeated four times. Finally, the wafers were heated at 650°C in a furnace for 10 minutes under oxygen flow. The final thickness of the PLZT films was around 200 nm. The PLZT thin films were also prepared on platinum (Pt) coated MgO substrates with the (001) orientation taken as the reference of polarization. The Pt thin film was prepared by radio frequency (RF) sputtering at 650°C and was grown epitaxially on the MgO substrate.

For the top electrode, a Pt thin film was prepared by RF sputtering the PLZT thin films at room temperature. The top electrode was 200 μm in diameter and 150 nm thick. After sputtering, the silicon wafers with the top electrodes were an-

nealed again at 600°C for 1 hour under an oxygen flow.

The phases and the orientations of the thin films were determined by X-ray diffraction (XRD, X'pert-Pro MPD, Philips). The microstructures of the thin films were observed with a transmission electron microscope (H-9000NAR, Hitachi). The D-E hysteresis loop of the PLZT thin film was measured with a ferroelectric tester in virtual ground mode (RT6000HS, Radiant).

3. Results and discussion

Figure 1 shows the 2theta-theta XRD profile of the PLZT3/45/55 thin film grown on the SRO/CeO_2/YSZ multilayer structure on the (001) silicon substrate. No peaks were detected except for the (00*l*) peak. This indicates that the PLZT, SRO, CeO_2, and YSZ thin films were oriented toward the (001) direction, which is perpendicular to the surface of the substrate.

Figure 2 shows the XRD pole profiles (in-plane measurement) of the PLZT3/45/55 thin films on the SRO/CeO_2/YSZ structure on the (001) silicon substrate. The profiles show four poles corresponding to the (*l*0*l*) plane, indicating that the films grew epitaxially and have ø-scan patterns with a fourfold rotational symmetry. The rotation angle ø of the (202) peak of YSZ and CeO_2 coincides with that of silicon. This indicates that each layer grew epitaxially with a cube-on-cube alignment on the silicon crystal. The (101) peaks of SRO and PLZT thin films with the perovskite structure are shifted 45° with respect to the YSZ, CeO_2, and silicon. This indicates that these perovskite compounds rotate 45° with respect to the fluorite structure of the CeO_2 crystal. The reason for this rotation is the difference between the lattice constants of the perovskite and fluorite structures. **Figure 3** shows a schematic diagram of the epitaxial relationship between the perovskite, fluorite, and diamond structures. The lattice constants of the fluorite and diamond structures are 0.51 nm of YSZ and 0.54 nm of silicon, respectively. The mismatch between the lattice constants of YSZ and silicon (–5.6%) is relatively small. However, the lattice constants of the per-

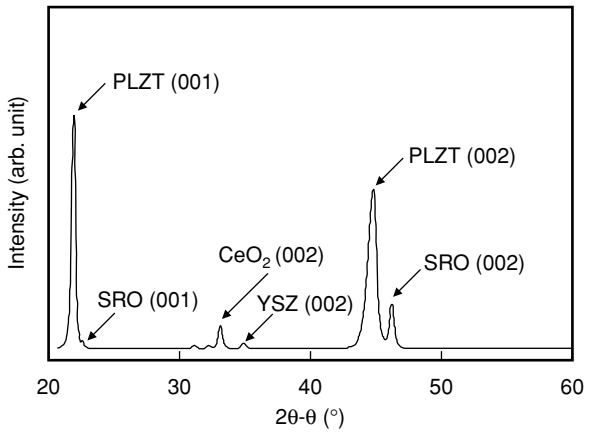

Figure 1
2θ-θ XRD profile of PLZT3/45/55 thin film grown on (001) silicon substrate with SRO/CeO_2/YSZ buffer layer.

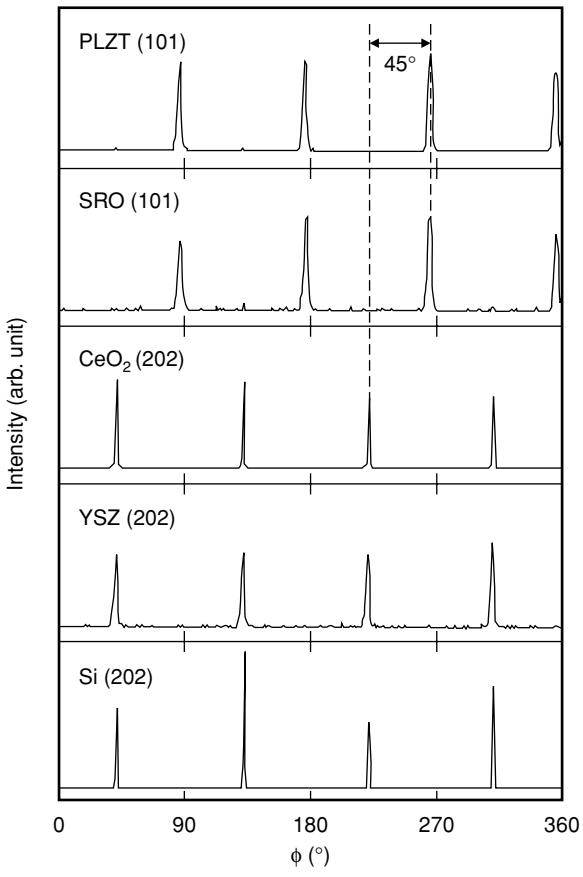

Figure 2
ϕ-scan XRD profiles of PLZT3/45/55 thin films grown on (001) silicon substrate with SRO/CeO_2/YSZ buffer layer.

ovskite and fluorite structures are 0.393 nm of pseudocubic SRO and 0.54 nm of CeO_2, respectively. The mismatch between the (100) direction of SRO and the (100) direction of CeO_2 is –27.2%, and the mismatch between the (110) direction of SRO and the (100) direction of CeO_2 is +2.9%. Because of these two mismatches, the distance between the (110) planes of the SRO is larger than the distance between the (100) planes of the CeO_2, and as a result, the SRO crystal is subjected to a compressive stress. This compressive stress is believed to increase the (001) orientation of the PLZT thin film, because the a-axis is shorter than the c-axis.

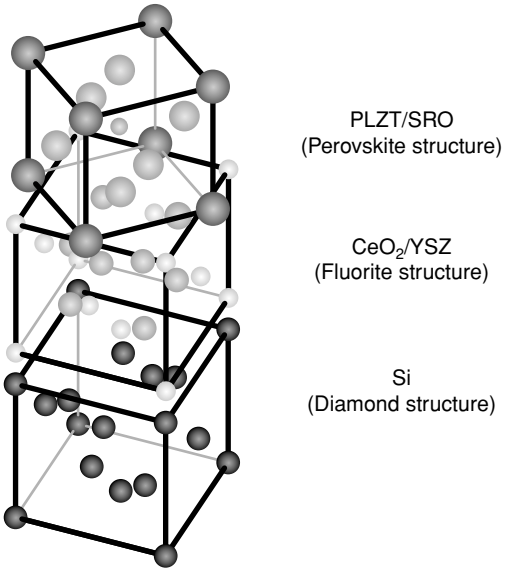

Figure 3
Schematic of the epitaxial relationships of PLZT/SRO/CeO_2/YSZ/Si(001) heteroepitaxial structure.

Figure 4 shows the microstructure of the PLZT3/45/55 thin film on the SRO/CeO_2/YSZ/Si heteroepitaxial structure. An amorphous SiO_2 layer (around 7 nm) was observed on the interface between the YSZ and silicon. This SiO_2 layer was formed by the diffusion of oxygen in the later process, because the growth of the YSZ thin film was influenced by the crystallinity of the silicon. No reactive phase was observed at the interfaces between the CeO_2-YSZ, CeO_2-SRO, and SRO-PLZT.

Figure 5 shows the D-E hysteresis loops of the epitaxial PLZT3/45/55 and PLZT3/20/80 thin films on the SRO/CeO_2/YSZ/Si structure and the epitaxial PLZT3/45/55 on the Pt/MgO structure. The remanent polarization of the PLZT3/45/55 on the silicon substrate is 10 μC/cm^2. The remanent polarization of the PLZT3/45/55 on the Pt/MgO is 42 μC/cm^2. The remanent polarization of the

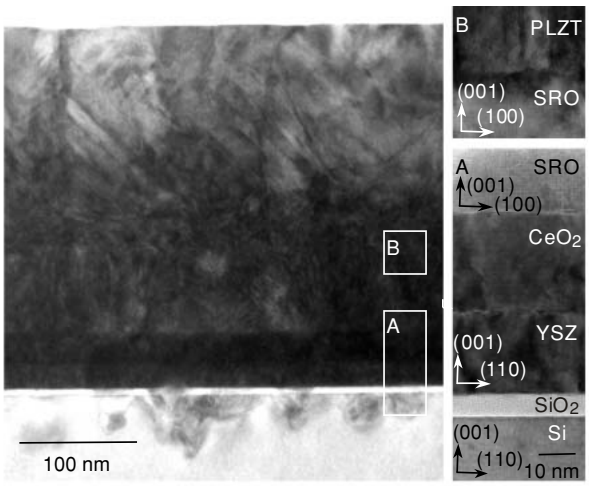

Figure 4
Cross-sectional microstructure of PLZT3/45/55/SRO/CeO_2/YSZ/Si(001) heteroepitaxial structure.

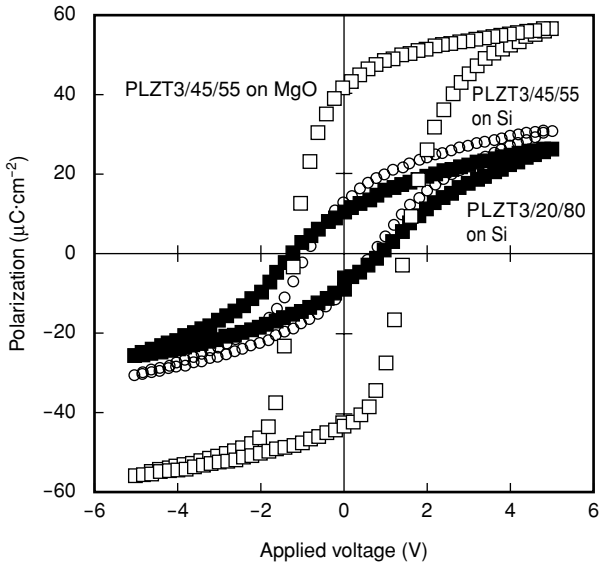

Figure 5
D-E hysteresis loops of PLZT3/45/55 on SRO/CeO_2/YSZ/Si and Pt/MgO and the PLZT3/20/80 thin films on the SRO/CeO_2/YSZ/Si heterostructure.

PLZT3/45/55 film on the silicon substrate is much smaller than that of the PLZT3/45/55 film on the Pt/MgO substrate.

The ratio of the c-axis to the a-axis of the lattice parameter increases with the amount of titanium in the PLZT. The remanent polarization of the PLZT3/20/80 thin film is expected to be larger than that of the PLZT3/45/55 thin film. However, the remanent polarization of the PLZT3/20/80 thin film is almost the same as that of the PLZT3/45/55 thin film. To understand this difference in the polarization properties of the PLZT thin films on the silicon and Pt/MgO substrates, the lattice parameters in and out of the plane of the PLZT film should be evaluated.

Figure 6 shows the reciprocal space mappings of the (204) planes of the PLZT3/45/55, PLZT3/20/80, and SRO thin films on the PLZT/SRO/CeO_2/YSZ/Si heterostructure. The (204) planes of the CeO_2 and YSZ thin films and the silicon substrate could not be detected, because they are rotated 45° in-plane with respect to the SRO and PLZT thin films, as shown in Figure 3. These profiles indicate the in-plane 90° domain structure of the PLZT thin film.

The in-plane and out-of-plane lattice parameters of each film and substrate are summarized in **Table 1**, and the lattice parameters of the PZT45/55, SRO, Pt, and MgO powders are summarized in **Table 2**. The lattice parameters of Pt and MgO coincide with the lattice constants of the powders. The crystal symmetry of the Pt thin film on the MgO substrate is cubic, because the

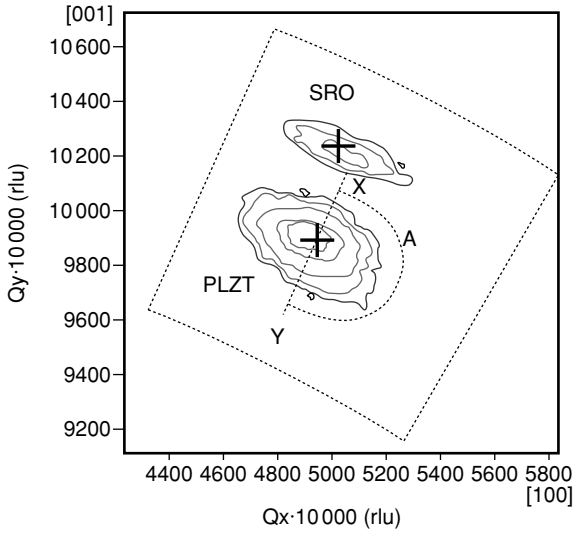

(a) PLZT3/45/55 on Si

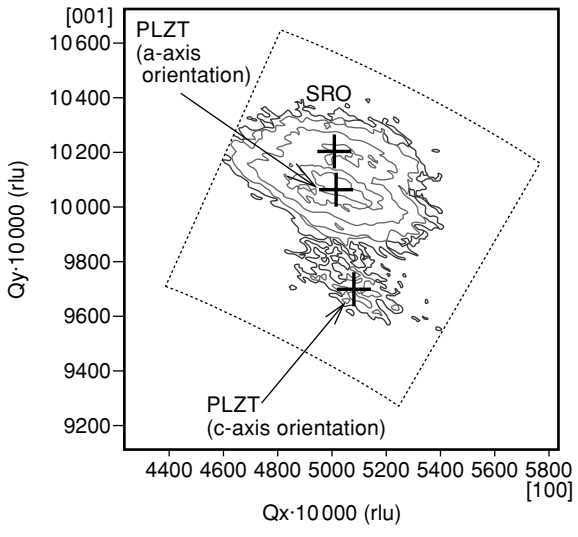

(b) PLZT3/20/80 on Si

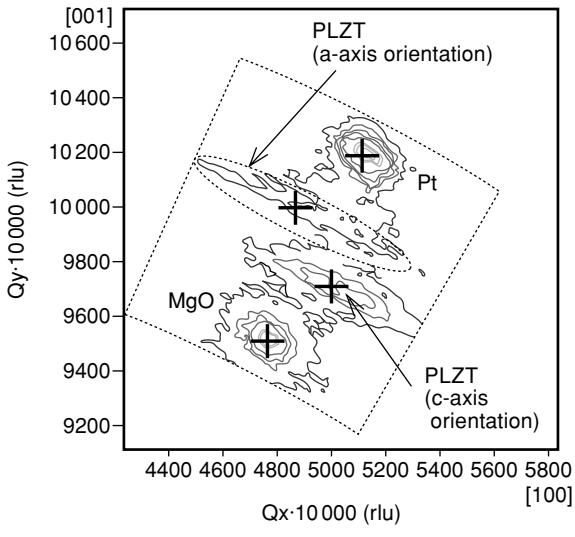

(c) PLZT3/45/55 on MgO

Figure 6
Reciprocal space mappings of the (204) planes of PLZT3/45/55, PLZT3/20/80, and SRO thin films on the PLZT/SRO/CeO_2/YSZ/Si heterostructure.

Table 1
Lattice parameters of PLZT, SRO, Pt, and MgO mapped in Figure 6.

Sample	PLZT (nm)					SRO (nm)		Pt (nm)		MgO (nm)	
	Pseudocubic		Tetragonal		c-orientation (Tetragonal: %)						
	in-plane	out-of-plane	in-plane	out-of-plane		in-plane	out-of-plane	in-plane	out-of-plane	in-plane	out-of-plane
PLZT 3/45/55 on Si	0.405	0.404	-	-	-	0.395	0.392	-	-	-	-
PLZT 3/20/80 on Si	0.399	0.392	0.395	0.411	18.1	0.398	0.397	-	-	-	-
PLZT 3/45/55 on Pt/MgO	-	-	0.401	0.412	76.5	-	-	0.392	0.392	0.420	0.420

Table 2
Lattice parameters of PLZT, SRO, Pt, and MgO powder.

Sample	PLZT45/55		SRO	Pt	MgO
	Tetragonal		Pseudocubic	Cubic	Cubic
	a (nm)	c (nm)	a (nm)	a (nm)	a (nm)
Lattice parameter	0.402	0.414	0.393	0.392	0.421

lattice parameter of the a-axis is the same as that of the c-axis. The Pt thin film is not distorted by the MgO substrate. The lattice parameters of the SRO thin films on the CeO_2/YSZ double buffer layer are slightly larger than those of the SRO powder and are spread out by the silicon substrate. The SRO thin film has a pseudocubic symmetry, because the in-plane lattice is almost the same as the out-of-plane lattice.

The lattice parameters of PLZT3/45/55 are different from those of the PZT45/55 powder.[16] The in-plane lattice parameters of the PLZT3/45/55 film are slightly larger than those of the out-of-plane lattice. These lattice parameters indicate that the PLZT3/45/55 thin film has a (100) orientation (a-axis orientation) with a pseudocubic structure. The X-Y line in Figure 6 (a) indicates that the in-plane and out-of-plane lattice parameters are equal. Area A indicates that the polarization of the lattice is perpendicular to the surface, because the out-of-plane lattice parameter is larger than the in-plane parameter. Thus, the lattices of area A contribute to the remanent polarization. The remanent polarization of the epitaxial PLZT3/45/55 thin film on silicon is smaller than that of the epitaxial films on Pt/MgO (Figure 5) because part of the crystal contributes to the remanent polarization. This contribution is due to the in-plane distortion that occurs in the PLZT thin film due to the tensile stress applied from the silicon substrate. The PLZT lattice becomes aligned with the silicon substrate at the crystallization temperature of 650°C. Around 600°C, the thermal expansion coefficient of the PLZT (6×10^{-6} K^{-1}) is larger than that of silicon (4×10^{-6} K^{-1}).[17] In the cooling process, the PLZT film contracts more than the silicon substrate. Thus, tensile stress is applied to the PLZT film from the silicon substrate. This tensile stress orients the PLZT film toward the (100) direction at the Curie temperature. Around 650°C, the thermal expansion coefficient of an MgO substrate (14×10^{-6} K^{-1}) is larger than that of the PLZT film.[17] Thus, compressive stress is applied to the PLZT film from the MgO substrate. This compressive stress orients the PLZT film toward the (001) direction at the Curie temperature. The component of (001) orientation (c-axis orientation) due to the compressive stress is 76.5%. The mismatch between the (101) direction of the perovskite and the (100) direction of the CeO_2 indicates that compressive stress has been applied. However, the results shown in Figures 5 and 6 indicate that the effect of the silicon substrate on the polarization is larger than that of the mismatch.

The PLZT3/20/80 has two peaks, one at a-axis orientation and another at c-axis orientation, because the ratio of the a-axis to the c-axis is larger than in PLZT3/45/55. The lattice parameters of the component of the a-axis orientation are 0.398 nm for the a-axis and 0.397 nm for the c-axis. The lattice parameters of the component of the c-axis orientation are 0.396 nm for the a-axis

and 0.411 nm for the c-axis. The component of the c-axis of PLZT increases with the amount of lead titanate. However, this indicates that most lattices of PLZT3/20/80 also have a pseudocubic structure. The stress affects the hysteresis of the PLZT thin film more than that of the composition. In the future, we plan to evaluate the imprint and the switching speed of this ferroelectric capacitor.

To improve the polarization property of epitaxial PLZT thin films on a silicon substrate, it is necessary to relax the tensile stress from the substrate and to increase the degree of (001) orientation, as described in this paper. We believe that the tensile stress can be relaxed by developing the buffer layer. In the future, we will also search for optimum materials for the epitaxial growth of perovskite films on silicon substrates.

4. Conclusions

This paper described the preparation of a PLZT/SRO/CeO_2/YSZ heteroepitaxial structure on a (001) silicon substrate and discussed the orientation of PLZT thin films on a SRO/CeO_2/YSZ buffer layer. All oxide thin films of the PLZT/SRO/CeO_2/YSZ heteroepitaxial structure were oriented toward (001). The CeO_2 and YSZ grew epitaxially with a cube-on-cube alignment with the diamond structure of the silicon. The PLZT and SRO thin films were rotated 45° in-plane with respect to the fluorite structure of the CeO_2. The remanent polarization of the PLZT3/45/55 epitaxial thin films was 10 μC/cm^2, which is smaller than that of a (001) oriented epitaxial film on an MgO substrate. The profiles of reciprocal space mapping reveal that the PLZT epitaxial thin films were distorted into a psudocubic structure by tensile stress from the silicon substrate. The findings described in this paper indicate many interesting areas for future investigations into epitaxial PLZT films, and we plan to develop the properties of these films on silicon substrates in the near future.

References

1) M. Suzuki: Review on Future Ferroelectric Nonvolatile Memory: FeRAM (in Japanese). *Journal of Ceramic Society of Japan*, **103**, 11, p.1099-1111 (1995).
2) J. L. Moll and Y. Tarui: A New Solid State Memory Resistor. *IEEE Transactions on Electron Devices*, **ED-10**, p.338-339 (1963).
3) E. J. Tarsa, L. L. McCormic, and J. S. Speck: Common Themes in the Epitaxial Growth of Oxides on Semiconductors. Material Research Society Symposium Proceeding, **341**, p.73-85 (1994).
4) M. Suzuki and T. Ami: A Proposal of Epitaxial Oxide Thin Film Structures for Future Oxide Electronics. *Material Science Engineering*, **B41**, p.166-173 (1996).
5) M. Ishida, I. Katakabe, T. Nakamura, and N. Ohtake: Epitaxial Al_2O_3 Films on Si by low-pressure Chemical Vapor Deposition. *Applied Physics Letters*, **52**, 16, p.1326-1328 (1988).
6) D. K. Fork, F. A. Ponce, J. C. Tramontana, and T. H. Geballe: Epitaxial MgO on Si(001) for Y-Ba-Cu-O Thin-film Growth by Pulsed Laser Deposition. *Applied Physics Letters*, **58**, 20, p.2294-2296 (1991).
7) A. Masuda, Y. Yamanaka, M. Tazoe, T. Nakamura, A. Morimoto, and T. Shimizu: Preparation and Crystallographic Characterizations of Highly Oriented Pb($Zr_{0.52}Ti_{0.48}$)O_3 films and MgO Buffer Layers on (100)GaAs and (100)Si by Pulse Laser Deposition. *Journal of Crystal Growth*, **158**, p.84-88 (1996).
8) H. Fukumoto, M. Yamamoto, Y. Osaka, and F. Nishiyama: Strain Measurements in Heteroepitaxial Yttria-stabilized Zirconia on Si by Ion Beam Channeling. *Journal of Applied Physics*, **67**, 5, p.2447-2449 (1989).
9) S. Y. Hou, J. Kwo, R. K. Watts, J.-Y Cheng, and D. K. Fork: Structure and Properties of Epitaxial $Ba_{0.5}Sr_{0.5}TiO_3/SrRuO_3/ZrO_2$ Heterostructure on Si Grown of Off-axis Sputtering. *Applied Physics Letters*, **67**, 10,

p.1387-1389 (1995).

10) C. A. Copetti, H. Soltner, J. Schubert, W. Zander, O. Hollricher, Ch. Buchal, H. Schultz, N. Tellmann, and N. Klein: High Quality Epitaxy of $YBa_2Cu_3O_{7-\delta}$ on Silicon-on-sapphire with the Multiple Buffer Layer YSZ/CeO_2. *Applied Physics Letters*, **63**, 10, p.1429-1431 (1993).
11) N. Wakiya, T. Yamada, K. Shinozaki, and N. Mizutani: Heteroepitaxial growth of CeO_2 Thin Film on Si(001) with an Ultra Thin YSZ Buffer Layer. *Thin Solid Films*, **371**, p.211-217 (2000).
12) R. Haakenaasen, D. K. Fork, and J. A. Golovchenko: High Quality Crystalline $YBa_2Cu_3O_{7-\delta}$ Films on Thin Silicon Substrates. *Applied Physics Letters*, **64**, 12, p.1573-1575 (1994).
13) Y. Li, S. Linzen, P. Seidel, F. Machalett, F. Schmidl, H. Schneidewind, T. Schmauder, R. Cihar, and S. Schaller: Epitaxial Growth of $YBa_2Cu_3O_{7-x}$ Thin Films on $CoSi_2$/Si Substrates with Combined CeO_2/YSZ Buffer Layers. Institution of Physical Conference Series, **148**, p.911-914 (1995).
14) L. Mechin, J.-C. Villegier, G. Rolland, and F. Laugier: Double CeO_2/YSZ Buffer Layer for the Epitaxial Growth of $YBa_2Cu_3O_{7-\delta}$ Films on Si(001) Substrates. *Physica C*, **269**, p.124-130 (1996).
15) A. Pignolet, S. Welke, C. Curran, S. Senz, and D. Hesse: Large Area Pulsed Laser Deposition of Bi-layered Ferroelectric Thin Films. *Journal of Korean Physical Society*, **32**, 2, p.S1476-S1480 (1998).
16) Joint Committee on Powder Diffraction Standard – International Centre for Diffraction Data, Powder Data File, Vol. 50, No. 0346.
17) T. Nakamura: Ceramics-to-Netsu (Ceramics and Heat) (in Japanese). ed. by T. Yamaguchi and H. Yanagida, Ceramic Science Series No. 6, Gihoudo Press, Tokyo, 1985, p.31-34.

Masao Kondo received the B.E., M.E., and Dr. degrees in Engineering of Inorganic Materials from Tokyo Institute of Technology, Tokyo, Japan in 1990, 1992, and 1995, respectively. He joined Fujitsu Laboratories Ltd., Atsugi, Japan in 1995, where he has been engaged in research and development of piezoelectric ceramics, piezoelectric actuators, and ferroelectric thin films. He is a member of the Japan Society of Applied Physics and the Ceramic Society of Japan.

Kenji Maruyama received the B.E. degree in Applied Physics from the University of Tokyo, Tokyo, Japan in 1981 and the Dr. degree in Material Science from Tohoku University, Sendai, Japan in 2000. He joined Fujitsu Laboratories Ltd., Atsugi, Japan in 1981 and did research on the crystal growth of narrow and wide band gap II-VI semiconductor materials and optoelectronic device applications. He is currently engaged in research and development of thin film ferroelectric materials for non-volatile memory applications. He is a member of the Institute of Electrical and Electronics Engineers (IEEE) and the Japan Society of Applied Physics.

Kazuaki Kurihara received the B.E. degree in Metallurgic Engineering and the M.E. degree in Materials Science from Tokyo Institute of Technology, Tokyo, Japan in 1979 and 1981, respectively. He joined Fujitsu Laboratories Ltd., Kawasaki, Japan in 1981, where he has been engaged in research and development of ceramic materials and components. He is a member of the Japan Society of Applied Physics and the Ceramic Society of Japan.